# OPTIMUM VENTILATION AND AIR FLOW CONTROL IN BUILDINGS

**17th AIVC Conference, Gothenburg, Sweden,
17-20 September, 1996**

# Modelling and assessing ventilation efficiency in an imperfectly mixed ventilated air space

Janssens K.[1,2], Berckmans D.[1,2], De Moor M.[1]

(1) Laboratory for Agricultural Buildings Research,
Catholic University of Leuven,
K. Mercierlaan 92,
B-3001 Heverlee,
Belgium

(2) National Fund for Scientific Research,
Belgium

**Synopsis**

To ensure indoor air quality an efficient ventilation system should provide fresh air in those parts of a room where it is required. To assess whether the ventilation system fulfils the main objective, different definitions of local ventilation efficiency (the local mean age of air, the local ventilation rate, the local purging flow rate and the local air exchange rate) are reported in literature. Tracer gas techniques (step up method, step down method and pulse method) and CFD-models are mostly used in research to identify the 3-D distribution of these ventilation parameters in a ventilated air space.
In our laboratory the 'local volumetric concentration of fresh air flow rate' [m3/s.m3] was introduced as a new ventilation parameter. A total amount of 90 step up experiments was performed in a laboratory test installation with a volume of 9 m3 [3×2×1.5m] to model the 3-D distribution of this ventilation parameter in relation to different values of the ventilation rate (120-300 m3/h) and the heat supply (0-400 Watt) as control inputs. In the main part of the paper some results are given of the modelled 3-D distribution of the 'volumetric concentration of fresh air flow rate' in the test installation. This distribution of fresh air flow rate is assessed in relation to the air flow pattern which is visualised by smoke experiments and quantified by image analysis and the Archimedes number.

**List of symbols**

| | | |
|---|---|---|
| $V$ | = | total ventilation rate through the test room [m3/h] |
| $Q$ | = | heat supplied by the heating element positioned just beneath the air inlet [Watt] |
| $Q_{in}$ | = | internal heat production in the test room [Watt] |
| $Q_{wall}$ | = | heat losses through the walls [Watt] |
| $T_o$ | = | temperature of the incoming air in the test room [°C] |
| $T_i$ | = | temperature in the 'well mixed zone' [°C] |
| $V_c$ | = | part of the total ventilation rate entering the 'well mixed zone' [m3/s] |
| $Vol_c$ | = | volume of the 'well mixed zone' [m3] |
| $v_c$ | = | volumetric concentration of fresh air flow rate in the 'well mixed zone' [m3/s.m3] |
| $Ar_c$ | = | corrected Archimedes number [-] |

## 1. Introduction

The main objective of a ventilation system is to provide fresh air in those parts of a room where it is required. To assess whether the ventilation system fulfils the main objective, different definitions of local ventilation efficiency are reported in literature [1,2]. The most important are the local mean age of air [s], the local ventilation rate [1/s], the local purging flow rate [m3/s] and the local air exchange rate [1/s]. Different techniques have been developed to identify the 3-D distribution of these ventilation parameters in a ventilated air space. Among these techniques tracer gas experiments (step-up method, step-down method and pulse method) are used in most cases. CFD-models are also used, but these models still have many technical and fundamental problems (immense computational power, validation problem, ...) as reported in [3].

## 2. Objectives

In our laboratory the 'local volumetric concentration of fresh air flow rate' [m3/s.m3] was introduced as a new ventilation parameter [4]. The main objective of this paper is to show that the modelled 3-D distribution of the 'local volumetric concentration of fresh air flow rate' can be assessed in relation to the measured and quantified air flow pattern in the test installation.

## 3. Method

In a laboratory test installation with a volume of 9 m3 [3×2×1.5m] 90 step up experiments were performed to model the 3-D distribution of this ventilation parameter in relation to different values of the ventilation rate (120-300 m3/h) and the heat supply (0-400 Watt) as control inputs [5].

### 3.1. Test installation

The laboratory test installation is presented in figure 1. It is a ventilated room (L=3m, W=1.5m and H=2m) with two control inputs: the ventilation rate V (120-300 m3/h) bringing cold air with temperature To=11°C in the test room and the heat Q (0-400 Watt) supplied by the heating element (13 in figure 1) positioned just beneath the air inlet. These control inputs determine the position of the incoming air jet in the ventilated room [6]. The other inputs in the test room are the internal heat production $Q_{in}$ (300 Watt) simulating the occupants and the wall losses $Q_{wall}$ which are minimised because of a second envelope surrounding the test installation. The test room is furthermore provided with 36 sensors positioned in a 3-D grid to measure the spatial and time related distribution of temperature. The sensor configuration is shown in figure 2. A more detailed description of the test installation is given in [5].

### 3.2. Definition of the 'local volumetric concentration of fresh air flow rate'

According to what has been shown in literature [4,7,8,9] and has been measured in the laboratory test installation [6], the air in the ventilated test room is considered to be not perfectly mixed in which there is a 3-D air flow pattern and related gradients in temperature. Although the air in the test room is not perfectly mixed, it is always possible to consider a 3-D **well mixed zone** around a local sensor position in which there is a better mixing and an acceptable gradient of temperature. The acceptable gradient of temperature in the well mixed zone is defined by the application (0.1°C for a micro-ship oven, 2°C for a greenhouse, 3°C for a livestock building,...). In the test room we furthermore consider an air flow pattern which brings only the part $V_c$ [m3/s] of the total ventilation rate V to the considered well mixed zone. Since the volume $Vol_c$ [m3] of the well mixed zone is unknown, the 'local volumetric concentration of fresh air flow rate' is considered as the local ventilation parameter in the well mixed zone and is defined as $v_c=V_c/Vol_c$ [m3/s.m3]. A graphical representation of this concept is shown in figure 3. It will be illustrated in section 4 that the 'local volumetric concentration of fresh air flow rate $v_c$ [m3/s.m3]' in a well mixed zone is varying as a function of the ventilation rate V [m3/h] and the heat supply Q [Watt] as control inputs and the corresponding air flow pattern. The 'local volumetric concentration of fresh air flow rate $v_c$ [m3/s.m3]' can therefore be considered as a useful local ventilation parameter.

### 3.3. Identification procedure

1. To identify the 'local volumetric concentration of fresh air flow rate $v_c$ [m3/s.m3]' in the considered well mixed zone in relation to the ventilation rate V [m3/h] and the heat supply Q [Watt], 90 step up experiments were performed in the test installation. During these experiments the ventilation rate V was varied step wise from 80 $m^3/h$ (900 sec.) to 120, 140, 160, 180, 200, 220, 240, 260, 280 or 300 $m^3/h$ (2700 sec.), resulting in an exponential decay of temperature in the considered well mixed zone. The control heat supply Q was set to 0 or 400 Watt. During each experiment the exponential decay of temperature was measured with a time step of 1 second using the local sensor in the considered well mixed zone. In the tables 1 and 2 an overview is given of the 90 performed step up experiments. In figure 4 one of the step up experiments together with the measured decay of temperature in sensor [431] is presented as an example. The position of this sensor can be found in figure 2.

2. Using the monitored values of temperature in the considered well mixed zone during a step up experiment, it becomes possible to identify the 'local volumetric concentration of fresh air flow rate $v_c$ [m3/s.m3]' in the well mixed zone corresponding to the ventilation rate V [m3/h] after the step and the applied heat supply Q [Watt]. Therefore, equation (1) can be used [10]:

$$v_c = \frac{1}{\int_{900}^{3600} \frac{Ti(t)-Ti_2}{Ti_1-Ti_2} dt} \quad (1)$$

in which:

| | | | |
|---|---|---|---|
| | $v_c$ | = | local volumetric concentration of fresh air flow rate [m3/s.m3] |
| | Ti(t) | = | measured temperature in the well mixed zone at time t [°C] |
| | $Ti_1$ | = | temperature in the well mixed zone at time step 900, just before the step on the ventilation rate [°C] |
| | $Ti_2$ | = | temperature in the well mixed zone at time step 3600 at the end of the experiment when steady-state is achieved [°C] |

As an example, equation (1) is applied to the measured temperature decay in sensor [431] as presented in figure 4. The equation returns for this particular experiment a $v_c$-value of 0.0102 m3/s.m3. This means that the 'local volumetric concentration of fresh air flow rate' in the well mixed zone around sensor [431] is 0.0102 m3/s.m3 when the ventilation rate V in the test room is 160 m3/h and there is no control heat supply Q.

3. By applying equation (1) to the 90 performed step up experiments in the test room, the 'local volumetric concentration of fresh air flow rate $v_c$ [m3/s.m3]' in the considered well mixed zone can be identified in relation to the different values of the ventilation rate V (120, 140, 160, 180, 200, 220, 240, 260, 280 and 300 $m^3/h$) and the control heat supply Q (0 and 400 Watt). In figure 5 an example is given of the identified relationship between the 'local volumetric concentration of fresh air flow rate $v_c$' in the well mixed zone around sensor [431] and the two control inputs V and Q. The 90 points on the figure represent the 90 performed step up experiments. The fitting curve is a second order polynomial.

4. The identification procedure has been used to identify the $v_c$/V,Q-relationships for the 36 sensor positions in the test installation. These relationships are given in [5]. From these relationships the 3-D distribution of the 'local volumetric concentration of fresh air flow rate' can be determined, and this for different values of the ventilation rate V (120-300 m3/h) and the heat supply Q (0-400 Watt) as control inputs. It will be shown in the next section that this 3-D distribution of fresh air flow rate can be related to the air flow pattern in the test room.

## 4. Results

It was hypothesized in the previous section that the 3-D distribution of the 'local volumetric concentration of fresh air flow rate $v_c$ [m3/s.m3]' can be related to the air flow pattern in the ventilated test room. To test this hypothesis the air flow pattern is first visualised and quantified for different values of the ventilation rate and the control heat supply. After that, the 3-D distribution of fresh air flow rate is related to the air flow pattern.

### 4.1. Visualisation and quantification of the air flow pattern

To visualise the air flow pattern $TiCl_4$-smoke is injected in the incoming air and the air flow pattern is filmed with a camera. The position of the air flow pattern is thereafter quantified by calculating the co-ordinates of the centreline of the air flow pattern [6]. The position of the air flow pattern can also be quantified by calculating the corresponding Archimedes number $Ar_c$ [11]. According to Randall and Battams [11] three categories of air flow patterns can be distinguished as a function of the Archimedes number $Ar_c$: a horizontal air flow pattern ($Ar_c<30$), an unstable air flow pattern ($30<Ar_c<75$) and a falling air flow pattern ($75<Ar_c$). These categories of air flow patterns can also be generated in the laboratory test installation.
Nine experiments were performed in the test room to visualise and quantify the air flow pattern for different values of the ventilation rate V [m3/h] and the heat supply Q [Watt]. An overview of these experiments is given in table 3. Some of the results are presented in the figures 6 and 7. In figure 6 the centreline of the incoming air jet is visualised for ventilation rates of 88, 158, 249 and 308 m3/h. The corresponding Archimedes numbers are also calculated and presented in this figure. It can be seen from this figure that the three categories of air flow patterns are generated in the test room and that the above criterium of Randall and Battams is confirmed. In figure 7 the 2-D centreline of the incoming air jet is visualised for a control heat supply Q of 0 and 400 Watt.

### 4.2. Physical interpretation of the $v_c$/V,Q-relationships

In general it can be concluded from the figures 6 and 7 that a higher ventilation rate or control heat supply results in an upward deflection of the air flow pattern. This influence of the ventilation rate and the control heat supply on the position of the air flow pattern is reflected in the $v_c$/V,Q-relationships of the 36 sensor positions in the test room. The $v_c$/V,Q-relationship of sensor position [431] is interpreted here as an example. This relationship is given in figure 5. The position of sensor [431] can be found in the figures 2, 6 and 7. It can be seen from the $v_c$/V,Q-relationship in figure 5 that a higher ventilation rate V [m3/h] yields a higher $v_c$-value in the well mixed zone around sensor [431]. This can be explained, because a higher ventilation rate brings more fresh air in the whole ventilated room and results in an upward deflection of the air flow pattern so that more fresh air moves towards the considered well mixed zone around sensor [431]. It can also be seen that a heat supply Q of 400 Watt yields a higher $v_c$-value in the well mixed zone around the considered sensor. This is again due to the air flow pattern which is found upward because of the heat supply Q.

### 4.3. Physical interpretation of the 3-D distribution of the 'volumetric concentration of fresh air flow rate $v_C$'

From the 36 identified $v_C$/V,Q-relationships in the test installation the 3-D distribution of the 'local volumetric concentration of fresh air flow rate $v_C$ [m3/s.m3]' can be determined by linear interpolation, and this for different values of the ventilation rate (120-300 m3/h) and the heat supply (0-400 Watt). In figure 8 the distribution of the 'local volumetric concentration of fresh air flow rate $v_C$ [m3/s.m3]' is visualised in the front and the rear plane of sensors when the ventilation rate V is 180 m3/h and the heat supply Q is 400 Watt. From these figures it can be seen that most of the fresh air flows in the upper regions of the test installation. This is due to the air flow pattern which is found upward because of the buoyancy force on the air jet caused by the control heat supply Q.

## 5. Conclusions

The 'local volumetric concentration of fresh air flow rate $v_C$ [m3/s.m3]' has been introduced as a new ventilation parameter. A total amount of 90 step up experiments was performed in a laboratory test installation [3×2×1.5m] to model the 3-D distribution of this ventilation parameter in relation to different values of the ventilation rate (120-300 m3/h) and the heat supply (0-400 Watt) as control inputs. From the results it can be confirmed that the 3-D distribution of the 'volumetric concentration of fresh air flow rate' can be assessed in relation to the air flow pattern which has been visualised by smoke experiments and quantified by image analysis and the Archimedes number $Ar_C$.

## 6. References


[1] Sandberg M., 1981. What is ventilation efficiency? Building and Environment, Vol.16, No.2, p.123-135.

[2] Sandberg M. and Sjöberg M., 1983. The use of moments for assessing air quality in ventilated rooms. Building and Environment, Vol.18, No.4, p.181-197.

[3] De Moor M. and Berckmans D., 1994. Modelling the heat and mass transfer in a ventilated air space by using a grey box modelling approach. Proceedings of Roomvent '94, Krakow, Poland, June 15-17, 1994, Vol. 1, p.185-204.

[4] Berckmans D., 1986. Analyse van de klimaatbeheersing in dierlijke productie-eenheden ter optimalisering van de regeling. PhD. Thesis, K.U.Leuven, pp. 376.

[5] De Moor M., 1996. Modelling and control of energy and mass transfer in imperfectly mixed fluids. PhD. Thesis, K.U.Leuven, pp. 269.

[6] De Moor M. and Berckmans D., 1993. Visualisation of measured three-dimensional well mixed zones of temperature in a ventilated space. 14th AIVC Conference on Energy Impact of Ventilation and Air Infiltration, Copenhagen, Denmark, Sept. 21-23, 1993.

[7] Randall J.M., 1979. The prediction of air flow pattern in livestock buildings. J. Agric. Build. Res., Vol. 20, p.199-215.

[8] Randall J.M., 1981. Ventilation system design. Environmental Aspects of Housing for Animal Production. Clark J.A. Butterwords, London, p.351-369
[9] Timmons M.B., 1980. Use of models to predict fluid flow motion in mechanically ventilated spaces. ASAE-paper n° 80-4018, 31 pp.
[10] Janssens K., 1995. Modelleren van energie- en massatransferten in niet perfect gemengde luchtmengsels. Eindverhandeling voorgedragen tot het behalen van de graad van Bio-Ingenieur in de Landbouwkunde, K.U.Leuven, pp. 94.
[11] Randall J.M. and Battams V.A., 1979. Stability criteria for air flow patterns in livestock buildings. J. Agric. Engng. Res., Vol. 24, p.361-374.

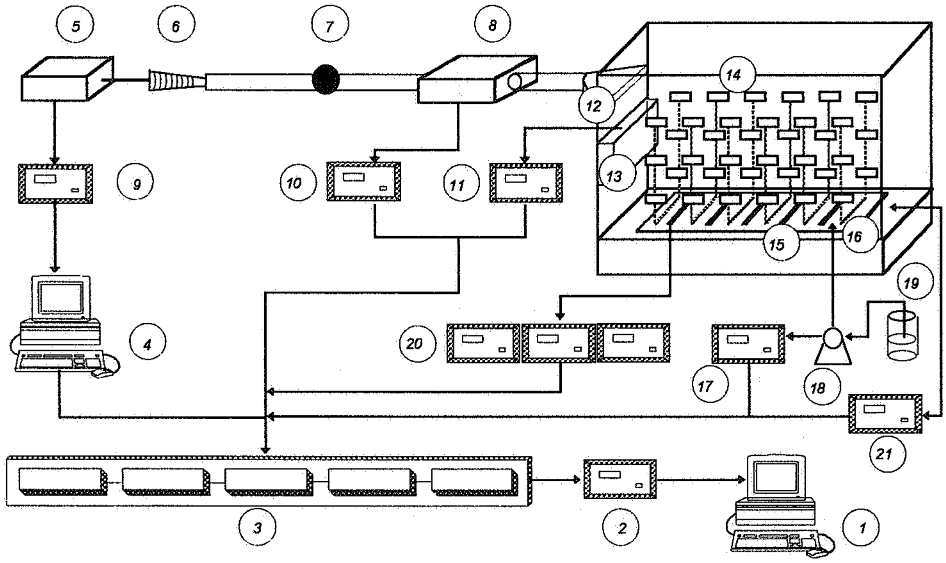


**1.** Minicomputer (monitor, floppy disc, to store and visualise the measured data). **2.** Parallel-interface for digital and analogue signals. **3.** Scan- and measurement unit. **4.** Minicomputer (to control and measure the produced air flow rate). **5.** Stepmotor to control the position of the cone, used as diaphragm. **6.** Cone, used as diaphragm, to produce the desired air flow rate. **7.** Centrifugal fan, to generate a ventilating rate. **8.** Cooling installation to control the inlet temperature. **9.** Differential pressure transducer to measure pressure difference between the test chamber and the envelope. **10.** Control- and measurement unit of the cooling installation. **11.** Control- and measurement unit of the heating element. **12.** Air inlet (slot inlet). **13.** Heating element. **14.** Three dimensional grid of temperature and humidity sensors. **15.** Aluminium semi conductor heat sinks to provide internal heat production. **16.** Undeep water reservoir with a streamer containing hot water to generate the internal moisture production. **17.** Unit to control and measure the amount of water supplied to the undeep water reservoir. **18.** Water pump. **19.** Water supply reservoir. **20.** Power supplies for internal heat production. **21.** Pressure difference measurement used to control the outlet fan.

**Figure 1**: Schematic representation of the laboratory test installation (L=3m, W=1.5m, H=2m).

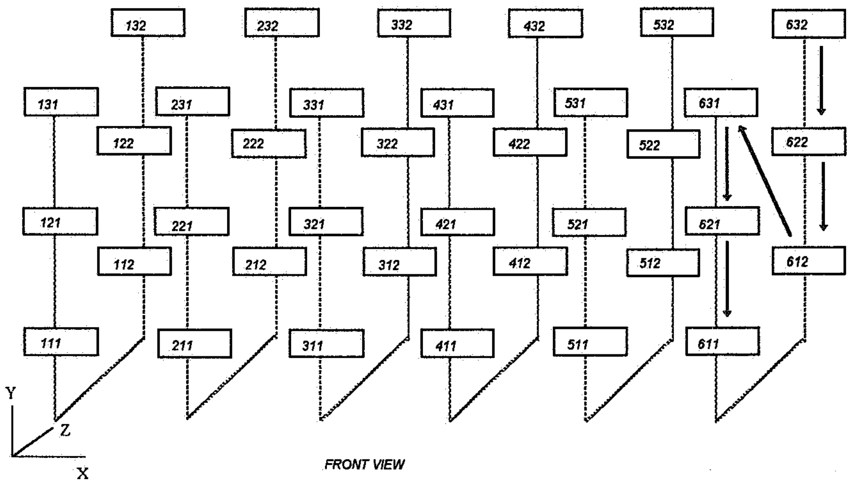


**Figure 2**: Sensor configuration in the test installation

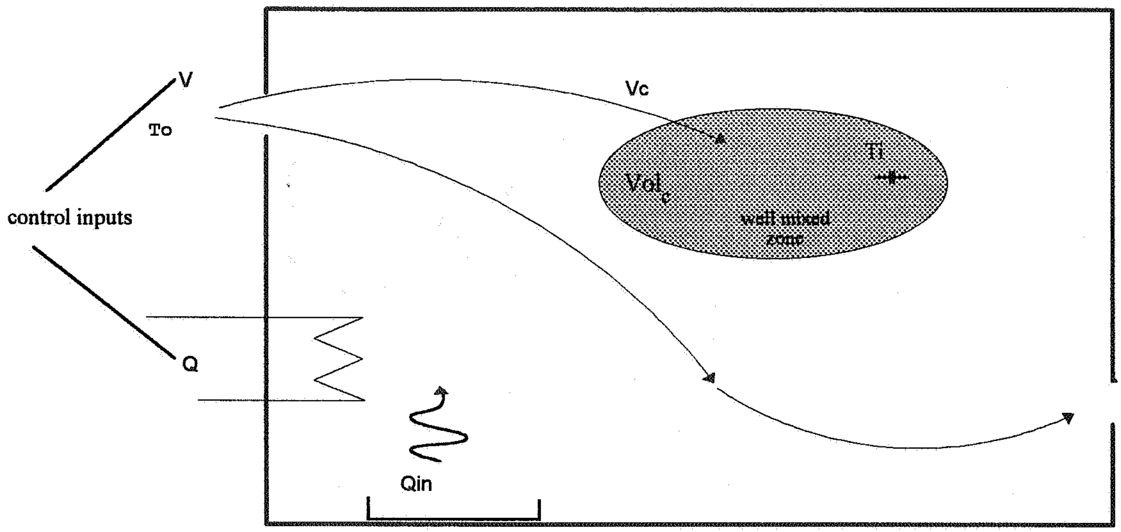


**Figure 3**: Graphical representation of the concept: the 'local volumetric concentration of fresh air flow rate $v_C = V_C/Vol_C$'

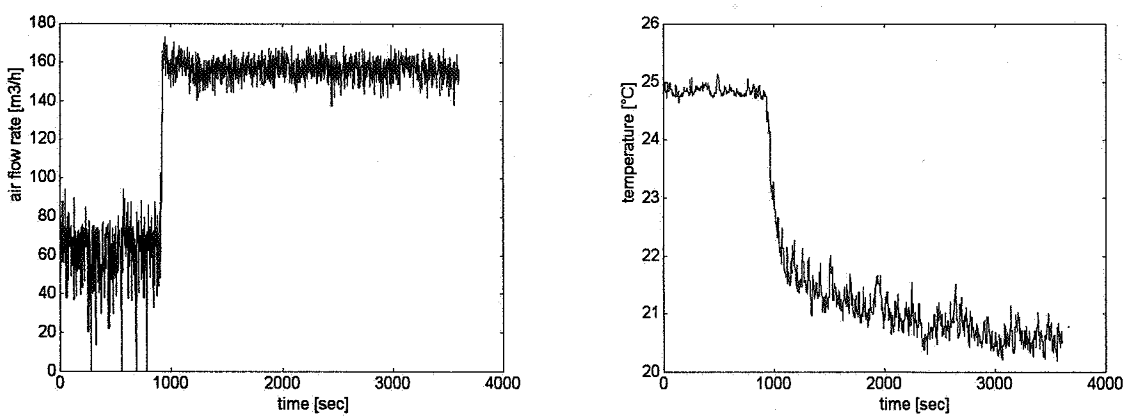


**Figure 4** : The ventilation rate V [m3/h] during a step up experiment. The heat supply Q is set to 0 Watt (left). The measured decay of temperature in sensor [431] during the step up experiment (right).

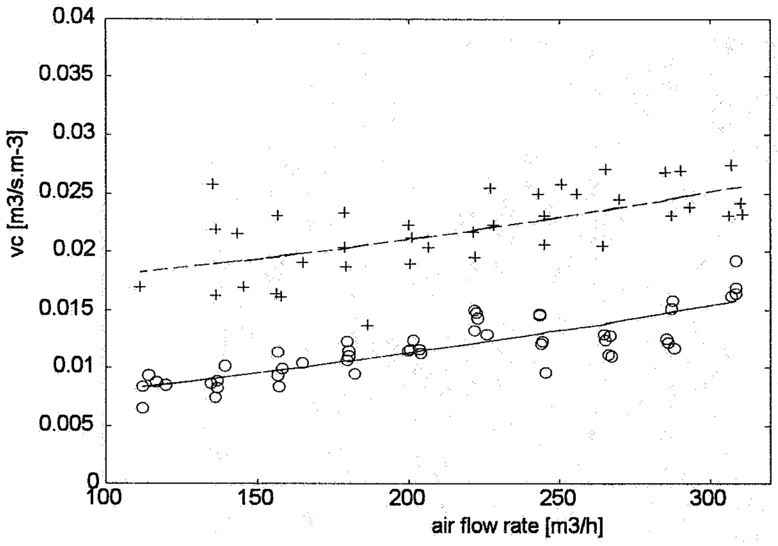


**Figure 5**: The $v_c$/V,Q-relationship for sensor position [431].
('+' = 400 Watt, 'o' = 0 Watt)

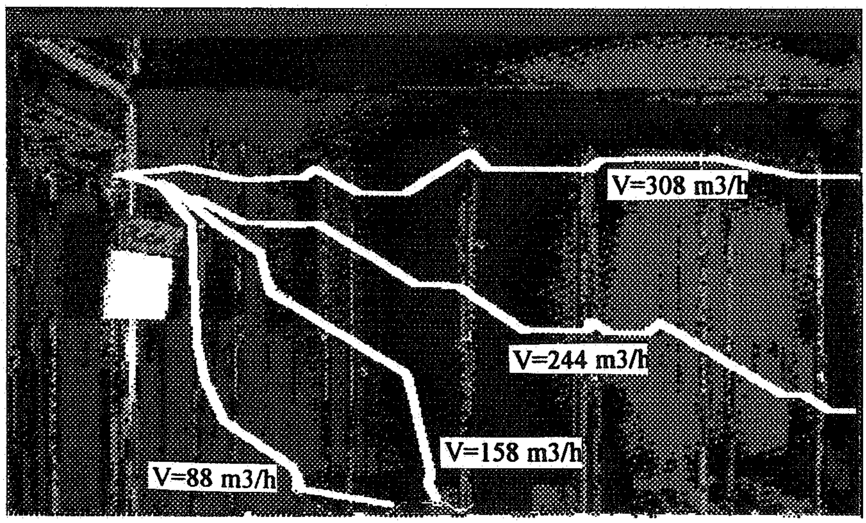


**Figure 6**: The centreline of the incoming air jet for different ventilation rates and corresponding Archimedes numbers:

(1) V=88 m3/h, $Ar_c$=393, falling air flow pattern
(2) V=158 m3/h, $Ar_c$=111, falling air flow pattern
(3) V=244 m3/h, $Ar_c$=42, unstable air flow pattern
(4) V=308 m3/h, $Ar_c$=24, horizontal air flow pattern

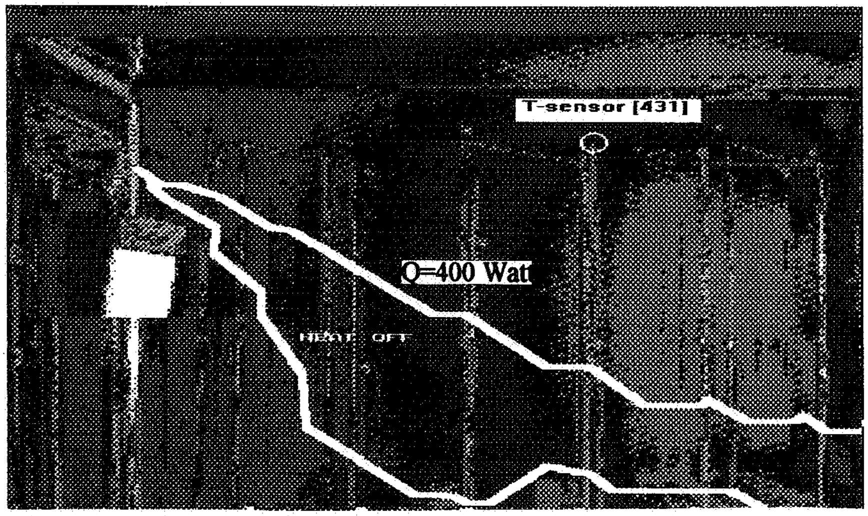


**Figure 7:** The centreline of the incoming air jet for a ventilation rate V=148 m3/h with heat supply Q=400 Watt and without heat supply Q.

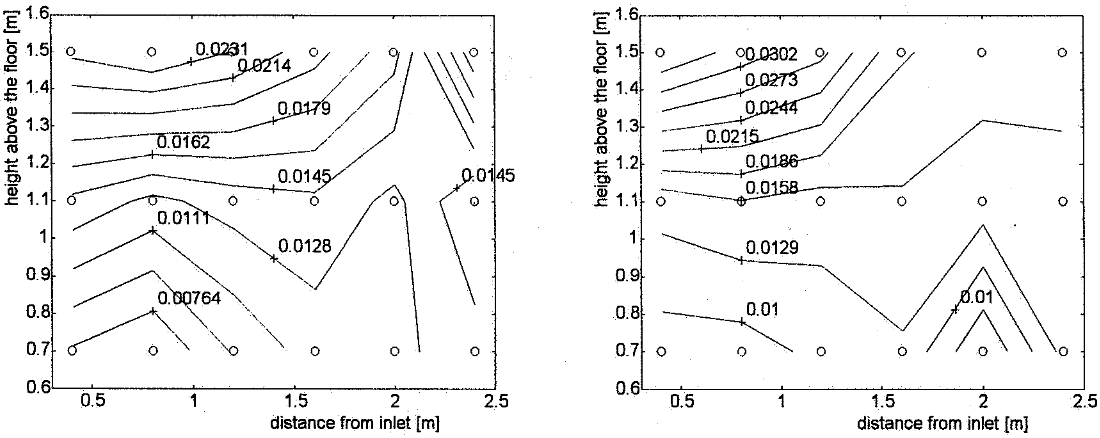


**Figure 8**: The distribution of the 'volumetric concentration flow of fresh air $v_C$ [m3/s.m3]' in the front plane of sensors (left figure) and the rear plane of sensors (right figure) for a ventilation rate V of 180 m3/h and a control heat supply Q of 400 Watt. The lines represent iso-$v_C$, the 'o' represent the 18 sensors in a plane.

| file name | *V* begin [m3/h] | *V* end [m3/h] | Q [Watt] | To [°C] |
|---|---|---|---|---|
| me0510ta | 63.78 | 112.32 | 0 | 11.55 |
| me1210ta | 54.52 | 112.06 | 0 | 11.22 |
| me2210ta | 59.27 | 136.57 | 0 | 11.83 |
| me0511ta | 62.34 | 117.06 | 0 | 11.99 |
| me1611ta | 71.47 | 119.87 | 0 | 11.67 |
| me0510tb | 59.83 | 136.65 | 0 | 11.77 |
| me1310ta | 59.11 | 134.92 | 0 | 11.35 |
| me2210tb | 60.26 | 136.43 | 0 | 11.97 |
| me0511tb | 62.52 | 114.12 | 0 | 12.22 |
| me1611tb | 66.82 | 139.34 | 0 | 11.89 |
| me0610ta | 57.03 | 157.20 | 0 | 11.80 |
| me1310tb | 61.24 | 156.44 | 0 | 11.52 |
| me2210tc | 60.74 | 158.31 | 0 | 11.96 |
| me0611tb | 58.18 | 156.79 | 0 | 12.44 |
| me1911ta | 78.10 | 165.06 | 0 | 11.69 |
| me0610tb | 64.12 | 180.32 | 0 | 12.33 |
| me1310tc | 53.80 | 179.57 | 0 | 11.65 |
| me2610ta | 62.67 | 179.84 | 0 | 12.03 |
| me0911ta | 57.07 | 180.01 | 0 | 12.13 |
| me1911tb | 64.59 | 182.41 | 0 | 11.67 |
| me0610tc | 58.38 | 200.80 | 0 | 12.37 |
| me1410ta | 28.72 | 200.15 | 0 | 11.60 |
| me2610tb | 72.12 | 204.14 | 0 | 12.09 |
| me0911tb | 58.68 | 201.43 | 0 | 12.43 |
| me2011ta | 63.64 | 203.81 | 0 | 11.80 |
| me0710ta | 61.39 | 221.98 | 0 | 12.02 |
| me1410tb | 58.86 | 222.59 | 0 | 11.71 |
| me2810ta | 57.97 | 223.25 | 0 | 12.10 |
| me1011ta | 58.23 | 222.14 | 0 | 12.15 |
| me2011tb | 67.11 | 226.00 | 0 | 11.96 |
| me0710tb | 54.72 | 243.51 | 0 | 12.39 |
| me1410tc | 58.59 | 244.40 | 0 | 11.79 |
| me2910ta | 56.76 | 243.76 | 0 | 12.14 |
| me1011tb | 53.47 | 243.25 | 0 | 12.32 |
| me2211ta | 70.15 | 245.45 | 0 | 11.85 |
| me0810ta | 59.86 | 264.63 | 0 | 12.03 |
| me1510ta | 61.12 | 267.41 | 0 | 12.00 |
| me2910tb | 56.52 | 265.41 | 0 | 12.40 |
| me1011tc | 59.44 | 267.14 | 0 | 12.08 |
| me2211tb | 67.92 | 266.25 | 0 | 12.04 |
| me0810tb | 54.83 | 285.92 | 0 | 12.36 |
| me1510tb | 54.15 | 288.57 | 0 | 12.19 |
| me2910tc | 59.36 | 286.42 | 0 | 12.59 |
| me1111ta | 66.83 | 287.76 | 0 | 12.18 |
| me2211tc | 66.82 | 287.18 | 0 | 12.21 |
| me0810tc | 55.71 | 307.28 | 0 | 12.50 |
| me1510tc | 51.22 | 308.91 | 0 | 12.26 |
| me2910td | 62.75 | 308.70 | 0 | 12.70 |
| me1111tb | 58.92 | 308.82 | 0 | 12.30 |
| me2311ta | 51.22 | 308.91 | 0 | 11.79 |

**Table 1:** 50 step up experiments with variable ventilation rate (Q=0 Watt)

| file name | *V* begin [m3/h] | *V* end [m3/h] | Q [Watt] | To [°C] |
|---|---|---|---|---|
| meqv16t1 | 76.02 | 155.96 | 400 | 12.17 |
| meqv14t1 | 76.87 | 135.17 | 400 | 12.33 |
| meqv18t1 | 63.07 | 178.43 | 400 | 11.99 |
| meqv20t1 | 55.26 | 199.90 | 400 | 12.04 |
| meqv22t1 | 48.88 | 221.40 | 400 | 11.69 |
| meqv24t1 | 68.03 | 244.93 | 400 | 11.88 |
| meqv26t1 | 63.13 | 255.80 | 400 | 12.01 |
| meqv28t1 | 68.76 | 287.43 | 400 | 11.94 |
| meqv30t1 | 54.39 | 306.00 | 400 | 11.87 |
| meqv12t1 | 64.46 | 111.47 | 400 | 11.42 |
| meqv15t2 | 55.01 | 145.28 | 400 | 11.24 |
| meqv20t2 | 51.79 | 200.78 | 400 | 11.57 |
| meqv26t2 | 76.91 | 269.90 | 400 | 11.77 |
| meqv30t2 | 76.45 | 310.78 | 400 | 11.57 |
| meqv28t2 | 76.80 | 290.44 | 400 | 11.64 |
| meqv24t2 | 79.95 | 250.33 | 400 | 11.41 |
| meqv22t2 | 75.16 | 227.92 | 400 | 11.44 |
| meqv18t2 | 75.64 | 186.40 | 400 | 11.33 |
| meqv16t2 | 79.13 | 165.08 | 400 | 10.85 |
| meqv14t2 | 79.87 | 143.60 | 400 | 11.30 |
| meqv20t3 | 76.14 | 206.48 | 400 | 11.63 |
| meav22t3 | 77.30 | 227.16 | 400 | 11.78 |
| meqv24t3 | 50.47 | 244.84 | 400 | 11.38 |
| meqv26t3 | 48.63 | 265.49 | 400 | 11.72 |
| meqv28t3 | 77.43 | 293.41 | 400 | 11.76 |
| meqv30t3 | 60.09 | 310.47 | 400 | 11.85 |
| meqv18t3 | 62.98 | 178.40 | 400 | 11.42 |
| meqv16t3 | 59.28 | 156.86 | 400 | 11.57 |
| meqv14t3 | 59.05 | 136.12 | 400 | 11.56 |
| meqv30t4 | 58.55 | 307.14 | 400 | 11.83 |
| meqv28t4 | 60.95 | 285.32 | 400 | 11.81 |
| meqv26t4 | 57.75 | 264.34 | 400 | 11.98 |
| meqv24t4 | 65.26 | 243.09 | 400 | 11.50 |
| meqv22t4 | 57.26 | 221.80 | 400 | 11.72 |
| meqv20t4 | 63.11 | 200.86 | 400 | 11.67 |
| meqv18t4 | 59.11 | 179.05 | 400 | 11.60 |
| meqv16t4 | 58.21 | 157.59 | 400 | 11.66 |
| meqv14t4 | 61.17 | 136.21 | 400 | 11.44 |
| meqv12t4 | 64.46 | 111.47 | 400 | 11.72 |

**Table 2:** 40 step up experiments with variable ventilation rate (Q=400 Watt)

| experiment | ventilation rate ($m^3/h$) | To (°C) | heat Q (W) | $Ar_c$-number | smoke |
|---|---|---|---|---|---|
| smoke 5 | 88 | 10.98 | 0 | 393 | $TiCl_4$ |
| smoke 6 | 124 | 11.05 | 0 | 212 | $TiCl_4$ |
| smoke 7 | 158 | 11.00 | 0 | 111 | $TiCl_4$ |
| smoke 8 | 201 | 11.11 | 0 | 65 | $TiCl_4$ |
| smoke 11 | 244 | 11.49 | 0 | 42 | $TiCl_4$ |
| smoke 13 | 286 | 11.51 | 0 | 29 | $TiCl_4$ |
| smoke 14 | 308 | 11.52 | 0 | 24 | $TiCl_4$ |
| smoke 15 | 101 | 10.9 | 0 | 298 | $TiCl_4$ |
| smoke 16 | 101 | 10.9 | 500 | - | $TiCl_4$ |

**Table 3:** Overview of the experiments to visualise and quantify the air flow pattern